Catal Lett (2008) 124:357–363
DOI 10.1007/s10562-008-9475-8

Oxidative Dehydrogenation of Ethylbenzene to Styrene with Carbon Dioxide over Fe_2O_3/TiO_2–ZrO_2 Catalyst: Influence of Chloride

Benjaram M. Reddy · Hailian Jin · Dae-Soo Han · Sang-Eon Park

Received: 12 February 2008 / Accepted: 3 March 2008 / Published online: 19 April 2008

Abstract This study was undertaken to know the influence of chloride ions in TiO_2–ZrO_2 mixed oxide and to explore chloride containing Fe_2O_3/TiO_2–ZrO_2 catalyst for oxidative dehydrogenation of ethylbenzene to styrene utilizing carbon dioxide as a soft oxidant. The TiO_2–ZrO_2 mixed oxide was synthesized by a co-precipitation method. Over the calcined support, a nominal 15 wt.% Fe_2O_3 was deposited by a wet impregnation method. The prepared catalysts were characterized using X-ray diffraction, temperature programmed desorption of NH_3 and CO_2, scanning electron microscopy and BET surface area methods. The catalytic activity measurements were made in a fixed-bed microreactor under normal atmospheric pressure. Characterization studies reveal that chloride ions exhibit a strong influence on the physicochemical and catalytic properties of the titania–zirconia composite oxides. The impregnated iron oxide was found to be in a highly dispersed form over the TiO_2–ZrO_2 support and influenced greatly on its acid–base properties. The chloride containing Fe_2O_3/TiO_2–ZrO_2 catalyst exhibited better activity and selectivity. The order of activity on various samples was found to be Fe_2O_3/TiO_2–ZrO_2 (chloride) > TiO_2–ZrO_2 (chloride) > TiO_2–ZrO_2.

Keywords Oxidative dehydrogenation · Ethylbenzene · Carbon dioxide · Styrene · TiO_2–ZrO_2 · Catalyst characterization

B. M. Reddy · H. Jin · D.-S. Han · S.-E. Park (✉)
Laboratory of Nano-Green Catalysis, Department of Chemistry, Inha University, Incheon 402-751, Republic of Korea
e-mail: separk@inha.ac.kr

B. M. Reddy
Inorganic and Physical Chemistry Division, Indian Institute of Chemical Technology, Hyderabad 500 007, India

1 Introduction

As enumerated by Smalley [1], the energy crisis and environmental pollution will be the first and foremost on the list of top 10 problems of humanity in the next 50 years. In particular, the global warming induced by an accelerative accumulation of carbon dioxide in the atmosphere is causing a lot of concern all over the world [2, 3]. Although carbon dioxide is considered as a discarded gas in the environmental field, it possesses a number of unique features that suggest utilization of CO_2 could provide both environmental and economical benefits [3]. One such method for its practical utilization is as a soft oxidant for catalytic selective oxidation or related reactions. Therefore, there is lot of interest on this subject ever since it was realized that CO_2 could be utilized as a soft oxidant for oxidative dehydrogenation (ODH) of various hydrocarbons including ethylbenzene (EB) to styrene and lower alkanes such as ethane, propane and butane to their value added alkene products [3–6]. Dissociation of CO_2 on the surface of an appropriate catalyst system easily produces active oxygen species. Therefore, several chemical reactions could benefit from using CO_2 as a mild oxidant, or as a selective source of active 'oxygen' species.

Styrene is an important monomer for several synthetic polymer materials in the petrochemical industry [7, 8]. Styrene is normally synthesized by two methods: mainly by an endothermic dehydrogenation of EB and as a co-product of propylene oxide production [7–10]. The ODH of EB is a third possibility to produce styrene employing different oxidants, which has gained a great deal of attention recently [4–6, 11–15]. The major advantage of the ODH process is that, unlike the endothermic dehydrogenation process, it can be operated at a lower temperature, as it is exothermic. Presently, more than 90% of styrene is

produced based on the catalytic dehydrogenation of EB at higher temperatures (>600 °C) employing promoted iron oxide catalysts in the presence of large excess of superheated steam [8, 10]. Due to endothermic and volume increasing nature of the reaction, a large amount of superheated steam is required to supply heat, shift the equilibrium to styrene, and avoid the formation of carbonaceous deposits [8]. This classical process thus consumes a large amount of energy, since all the latent heat of condensation is not recoverable at the gas–liquid separator after the reaction. Therefore, CO_2 has received a lot of attention as a soft oxidant or co-feed gas, instead of steam, since it will be in the gaseous form throughout the dehydrogenation process. The energy required for producing styrene employing steam and CO_2 were estimated to be 1.5×10^9 and 1.9×10^8 cal/t-styrene, respectively [13]. Therefore, the ODH process utilizing CO_2 could be considered as an energy-saving process. Further, application of CO_2 in the ODH process, for example, can encompass several advantages such as acceleration of the reaction rate, alleviation of the chemical equilibrium and enhancement in the product selectivity [4].

Recent investigations on the ODH of EB with CO_2 revealed that efficiency of this process is highly dependent on the nature of catalysts employed [5, 6]. Various catalyst systems based on Fe-, Cr- or V-oxides were investigated and some of them exhibited excellent catalytic properties for this reaction [4–6, 16–22]. Our recent studies revealed that titania-zirconia mixed oxides also exhibit excellent catalytic activity and selectivity for this reaction [6, 23, 24]. The TiO_2–ZrO_2 composite oxides received lot of attention recently as active catalysts as well as supports for a wide range of reactions [25]. The significant features of TiO_2–ZrO_2 mixed oxides include a high specific surface area, profound acid–base and redox properties together, a high thermal stability and strong mechanical strength [25]. During the course of our studies on this catalyst system, we realized that the presence of chloride impurity in the TiO_2–ZrO_2 mixed oxides exhibits a strong influence on its catalytic activity. The present study was undertaken to probe the influence of chloride in TiO_2–ZrO_2 mixed oxides on the conversion and selectivity of EB to styrene with CO_2 and to explore iron oxide impregnated TiO_2–ZrO_2 catalyst for this reaction. In this study, a chloride containing TiO_2–ZrO_2 (1:1 mole ratio) mixed oxide and a chloride free sample was synthesized under identical conditions following a coprecipitation method. On the calcined TiO_2–ZrO_2 support, a nominal 15 wt.% Fe_2O_3 was deposited by a wet impregnation method. The structural evolution of the synthesized catalysts was investigated using X-ray diffraction (XRD), temperature preprogrammed desorption (TPD) of NH_3 and CO_2, scanning electron microscopy (SEM) and BET surface area methods. The catalytic performance was evaluated for the ODH of EB to styrene in the vapor phase under normal atmospheric pressure employing CO_2 as the soft oxidant.

2 Experimental

2.1 Catalyst Preparation

The investigated TiO_2–ZrO_2 (1:1 mole ratio based on oxides) mixed oxide was synthesized by a coprecipitation method from $TiCl_4$ and $ZrOCl_2$ aqueous solutions by hydrolysis with ammonium hydroxide. In a typical experiment, the required quantities of zirconyl(IV) nitrate hydrate (Acros Organics, USA) and titanium(IV) chloride (Yakuri Pure Chemicals, Japan) were dissolved in deionized water and to which an aqueous ammonia (DC Chemicals, Korea) was added drop-wise with vigorous stirring until the precipitation was compete (pH = 7–8). The resultant precipitates were aged hydrothermally for 12 h at 100 °C before filtration. The well-formed white precipitates were separated into two equal portions and filtered under reduced pressure. To make the chloride-free TiO_2–ZrO_2 (TZ-1) sample, the precipitates were washed several times with deionized until free from chloride ions and the other portion was just filtered without washing to make the chloride containing TiO_2–ZrO_2 (TZ-2) sample. The resulting cakes were oven dried at 120 °C for 12 h and calcined at 550 °C for 6 h in air atmosphere. On the calcined TiO_2–ZrO_2 (TZ-2) sample, a nominal 15 wt.% Fe_2O_3 was deposited by adopting a standard wet impregnation method. For this purpose, the desired quantity of iron(II) chloride tetrahydrate (Aldrich, USA) was dissolved in deionized water, and the finely powdered calcined support was added with continuous stirring. The excess water was evaporated on a water-bath under vigorous stirring. The resulting material was oven dried at 120 °C for 12 h and subsequently calcined at 550 °C for 6 h in air atmosphere to obtain the final Fe_2O_3/TiO_2–ZrO_2 (FTZ) catalyst.

2.2 Catalyst Characterization

The total surface area and pore size distribution (BJH method) were determined using a multipoint BET method. Before analysis, samples were degassed at 250 °C under vacuum for 3 h. The measurements were carried out in a Micromeritics ASAP 2020 instrument using N_2 at liquid-nitrogen temperature. Powder X-ray diffraction patterns were obtained on a Rigaku Multiflex instrument using nickel-filtered Cu Kα (0.15418 nm) radiation source and a scintillation counter detector. The intensity data were collected over a 2θ range of 2–80° with a 0.02° step size and using a counting time of 1 s per point. The SEM images

were collected with a JEOL 630-F microscope. Before measurements, the powdered samples were dispersed on a steal plate surface and coated with Pt metal. The NH_3 and CO_2 TPD measurements were made on a Pulse Chemisorb 2705 (Micromeritics, USA) instrument. For these measurements, a high purity NH_3 or CO_2 gas was adsorbed at 100 °C for 30 min and purged at the same temperature with helium gas (20 mL/min) to remove the physisorbed gas. The TPD run was then conducted from 100 to 700 °C at a heating rate of 5 °C/min.

2.3 Catalyst Activity

The catalytic activity measurements were made in a fixed-bed down flow stainless steel microreactor (4.5 mm i.d. and 300 mm long) at normal atmospheric pressure [23]. For each catalytic run, ~1.0 g of sample was leaded in the centre of the reactor with the support of quartz wool plugs. The reactor assembly was heated to 600 °C at a heating rate of 2 °C/min in the flow of N_2 (20 mL/min) and kept at this temperature for 2 h. The N_2 was replaced with CO_2 (20 mL/min) and continued at the same 600 °C for 30 min preceding the reaction. The EB liquid was introduced into the preheating zone of the reactor through a motorized feed pump with a constant flow rate of 9.8 mmol/h. Gaseous and liquid products were analyzed simultaneously by an on-line gas chromatograph (Younlin Instrument, Acme 6000 Series, Korea) equipped with TCD and FID. A Porapak N 80/100 column (6 ft × 1/8″) and a HP-innowax column (30 m long, 0.32 mm i.d. and 0.25 μm film thickness) were employed for analysis of gaseous and liquid products, respectively. The main liquid products that were analyzed include styrene, benzene, toluene, benzaldehyde and acetophenone, and the gaseous products were hydrogen, methane, carbon monoxide and carbon dioxide.

3 Results and Discussion

The N_2 BET surface areas of various samples calcined at 550 °C are presented in Table 1. The chloride free TiO_2–ZrO_2 (TZ-1) mixed oxide sample exhibited a high specific surface area and pore volume. On the contrary, the chloride containing TZ-2 sample shows relatively less specific surface and pore volume. Of course, both TiO_2–ZrO_2 mixed oxides displayed more specific surface area than their individual component oxides, namely TiO_2 (15 m^2 g^{-1}) and ZrO_2 (25 m^2 g^{-1}), respectively [23]. The high specific surface areas of titania–zirconia mixed oxides are in conformity with their amorphous nature as observed from XRD and electron microscopy techniques described in the later paragraphs. A slight decrease in the specific surface area and pore volume is noted in the case of iron oxide impregnated TiO_2–ZrO_2 sample (FTZ). The decrease in the specific surface area after impregnating with Fe_2O_3 is due to various reasons, such as penetration of the deposited iron oxide into the pores of the support thereby narrowing its pore diameter and blocking some of the micropores, and solid-state reactions between the dispersed oxide and the supporting oxide [15]. The XRD results described in the subsequent paragraph strongly support the latter possibility.

Table 1 BET surface area and pore volume measurements of various samples calcined at 550 °C

Sample	Surface area (m^2 g^{-1})	Pore volume (mL g^{-1})
TiO_2–ZrO_2 (TZ-1)	207	0.65
TiO_2–ZrO_2 (TZ-2)	146	0.47
Fe_2O_3/TiO_2–ZrO_2 (FTZ)	132	0.41

The XRD profiles of the samples calcined at 550 °C are shown in Fig. 1. All samples exhibited broad diffraction patterns indicating amorphous nature of the materials. In particular, no XRD lines pertaining to crystalline ZrO_2 (monoclinic, tetragonal or cubic) and TiO_2 (anatase or rutile) phases were noted. Although it has been reported in the literature that tetragonal and monoclinic ZrO_2 and rutile TiO_2 could be formed at higher calcination temperatures, no such independent phases were noted in the present study [25]. However, The XRD patterns of the chloride containing TZ-2 and FTZ samples revealed some crystalline features of $ZrTiO_4$ compound [25]. Interestingly, no change in the XRD pattern of the TZ-2 support is noted after impregnating with iron oxide. Further, the XRD lines pertaining to any known or new crystalline compounds between Fe_2O_3 and TiO_2–ZrO_2 were observed. The XRD pattern after the reaction also exhibited no significant peaks corresponding to a composite

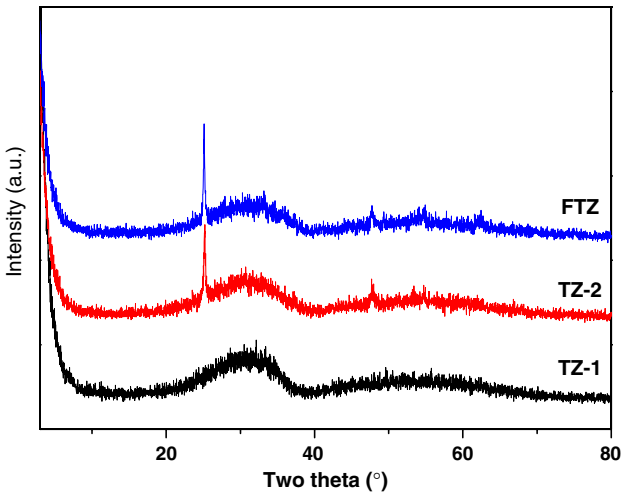

Fig. 1 X-ray powder diffraction patterns of TiO_2–ZrO_2 (TZ-1), TiO_2–ZrO_2 (TZ-2) and Fe_2O_3/TiO_2–ZrO_2 (FTZ) samples

oxide between iron and titania–zirconia. This observation reveals that bulk structure of the catalyst did not change during the reaction. The XRD results thus suggest that the impregnated iron oxide is in a highly dispersed form over the amorphous TiO_2–ZrO_2 composite oxide support.

The external morphologies of the samples were examined by SEM technique and the representative images are shown in Fig. 2. The SEM images reveal that all samples consist of typical spherical agglomerates with almost uniform size within the nanometer range. In particular, all samples exhibit good homogeneity. Interestingly, the TZ-1 sample exhibits amorphous features and the TZ-2 sample shows slightly better crystalline and sharp features in line with XRD results. Impregnation of iron oxide on the TiO_2–ZrO_2 mixed oxide did not reveal any significant changes in the external morphology of the sample. Coinciding with XRD results, the SEM results also support a high dispersion of iron oxide over the TiO_2–ZrO_2 support.

To distinguish the acid–base properties of these oxides, temperature programmed desorption of NH_3 and CO_2 were undertaken. The TPD measurements generally provide meaningful information about the available adsorption sites as well as the way in which the key species are chemisorbed on the catalyst surface. It is known that acidity and basicity of the catalysts often control the catalytic activity and selectivity in many acid–base catalyzed reactions [26]. The NH_3 TPD profiles of various samples are shown in Fig. 3. As defined in the literature, the amount of NH_3 desorbed below 200 °C is a measure of weak acidic sites, 200–350 °C range corresponds to medium acidic sites, and above 350 °C represents strong acid sites [27]. In the case of TZ-1 sample, a very broad desorption peak with its peak maximum is observed at around 245 °C. This peak is distributed in a wide temperature range from 200 to 450 °C with strong signal intensity. This strong and wide temperature range peak is primarily due to the generation of new acidic sites owing to mixing of TiO_2 and ZrO_2 leading to the formation Ti- and Zr- linkages through bridging oxygen bonds as described elsewhere [23, 25]. In addition to this intense board peak, a new broad peak is observed at 360 °C for TZ-2 sample. Intensity of this high temperature desorption peak increased slightly and shifted to a higher temperature for FTZ sample. Generation of these strong acidic sites in the TZ-2 and FTZ samples could be attributed to the presence of chloride ions and the dispersed iron oxide, respectively.

The CO_2 is an acidic gas; its adsorption on the catalyst surface is strongly influenced by the basic property of the solids. It can be assumed in principle that one CO_2 molecule adsorbs on one basic site of the catalyst. If the distribution of basic sites on the catalyst surface is uniform then it can be related to the number of basic sites of the catalysts. On the other hand, desorption temperature maximum (T_{max}) is a characteristic of the basic strength. The

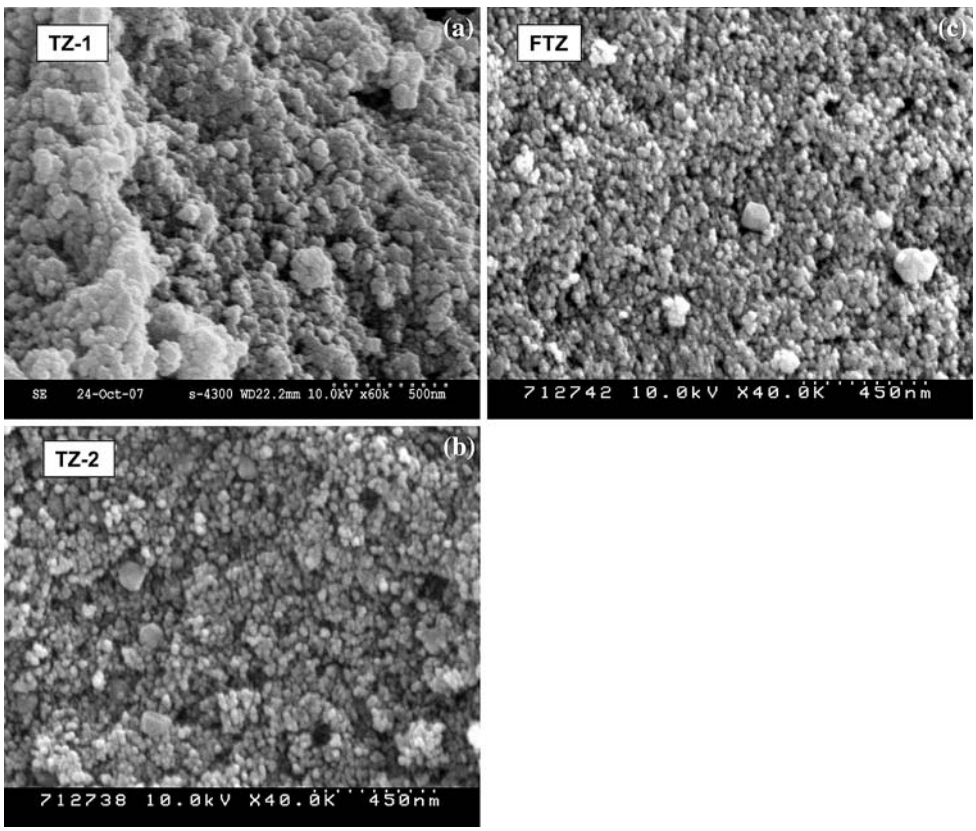

Fig. 2 SEM images of TiO_2–ZrO_2 (TZ-1), TiO_2–ZrO_2 (TZ-2) and Fe_2O_3/TiO_2–ZrO_2 (FTZ) samples

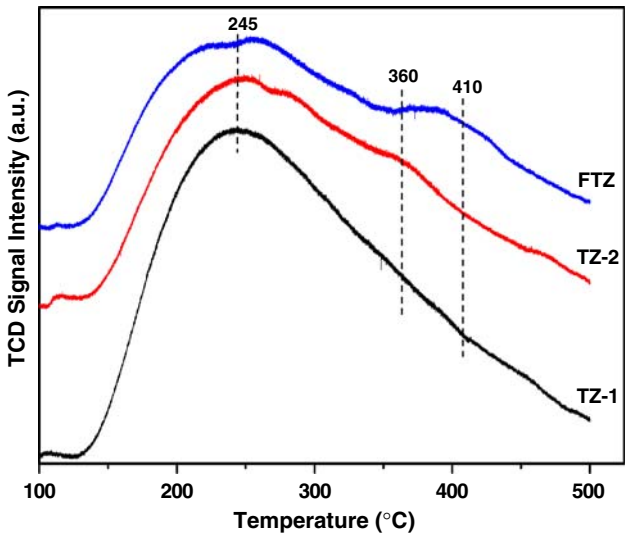

Fig. 3 The NH_3 TPD profiles of TiO_2–ZrO_2 (TZ-1), TiO_2–ZrO_2 (TZ-2) and Fe_2O_3/TiO_2–ZrO_2 (FTZ) samples

CO_2 TPD profiles of various samples are shown in Fig. 4. These exhibit a relatively broad desorption peaks with different peak maxima reflecting the acid–base properties. Although, the interpretation of CO_2 TPD profile is somewhat complex, a very similar NH_3 and CO_2 TPD profile, as noted in this study, was also reported for Li–Fe/Al samples by Dziembaj et al. [20]. In view of very board nature of the peaks, quantification of the peaks was not attempted in the present study. Of course, desorption peak maxima and resolution are highly dependent on the experimental conditions employed. The CO_2 TPD profile of TZ-1 sample is characterized by three peak maxima temperatures at ~200, 265 and 398 °C, respectively. The high temperature desorption peak maxima have been shifted to slightly lower temperatures in the case of TZ-2 and FTZ samples. Further, the TZ-2 and FTZ samples exhibited very board range of distribution unlike the TZ-1 sample. The shift in the high temperature desorption peak maxima to lower temperatures in the case of TZ-2 and FTZ samples could be due to the influence of chloride ions and the impregnated iron oxide, respectively. It is a known fact that chloride-containing materials exhibit more acidic properties than the chloride free samples [28]. A comparison of NH_3 and CO_2 TPD profiles of TiO_2–ZrO_2 mixed oxides with that of TiO_2 and ZrO_2 single oxides revealed an enhancement in the number and strength of both acidic and basic sites after mixing together [23].

The catalytic activity and selectivity results are presented in Fig. 5. In general, the conversion of EB increased with increasing reaction temperature and all catalysts exhibited a similar trend. However, for the purpose of better comparison, the catalytic activity data were generated at a constant temperature (600 °C) and optimum space velocity as described in the experimental section. The activity of the catalysts increased with time in the first few hours of the reaction and thereafter attained saturation. Therefore, for the purpose of comparison the catalytic data obtained after 4 h of reaction has been considered and presented in Fig. 5. The chloride containing TZ-2 sample exhibited a better conversion and product selectivity than that of chloride free TZ-1 sample. The FTZ combination

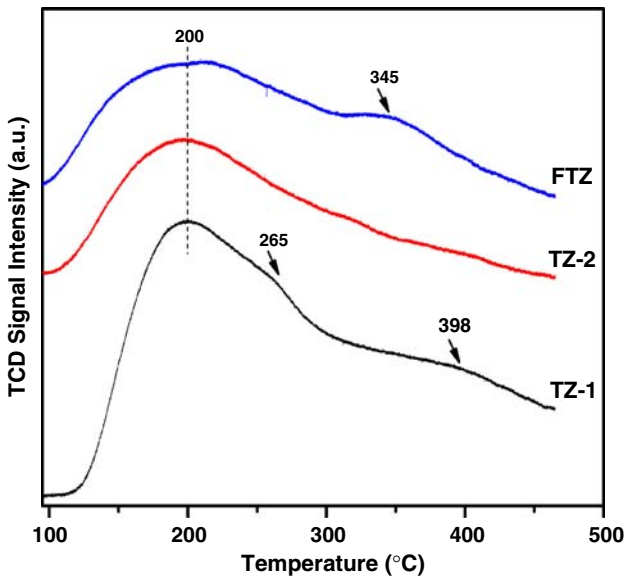

Fig. 4 The CO_2 TPD profiles of TiO_2–ZrO_2 (TZ-1), TiO_2–ZrO_2 (TZ-2) and Fe_2O_3/TiO_2–ZrO_2 (FTZ) samples

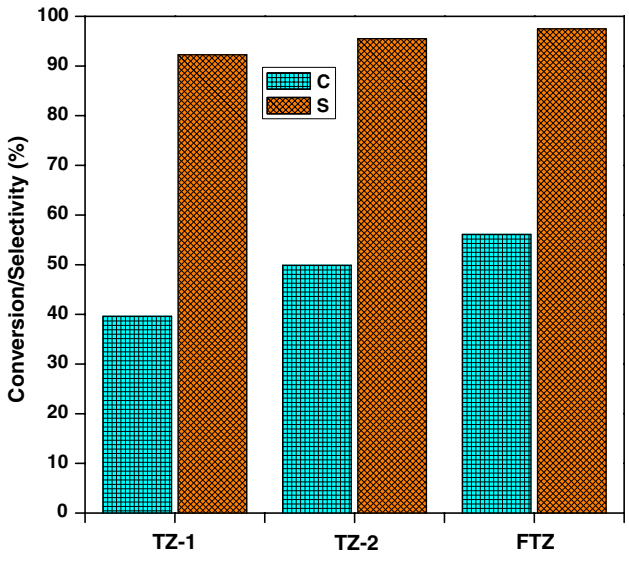

Fig. 5 Ethylbenzene conversion (C) and styrene selectivity (S) over TiO_2–ZrO_2 (TZ-1), TiO_2–ZrO_2 (TZ-2) and Fe_2O_3/TiO_2–ZrO_2 (FTZ) samples at 600 °C and normal atmospheric pressure

catalyst exhibited much better conversion and product selectivity than the other two samples. Our earlier study revealed that the TiO_2–ZrO_2 mixed oxide exhibits exceptionally better conversion and product selectivity than its individual component oxides (TiO_2 and ZrO_2) under identical reaction conditions [23]. The observed high catalytic activity and selectivity of TiO_2–ZrO_2 was proved to be due to the formation of an amorphous mixed oxide phase, enhancement in the specific surface area and an increase in the number and strength of acid–base sites [23, 25]. The origin of TiO_2–ZrO_2 composite oxide also appears to play an important role on its catalytic behavior. As noted from the present study, the presence of anion impurities alters the acid–base properties of the mixed oxides, which in turn exhibit influence on the catalytic behavior. Interestingly, the TiO_2–ZrO_2 mixed oxide (TZ-1) synthesized without chloride impurities exhibited a high specific surface area, but less active for the reaction.

A fast catalyst deactivation is often encountered on several catalysts in the dehydrogenation of EB to styrene [14]. Therefore, time-on-stream measurements are most significant to understand the behavior of various catalyst systems. As presented in Fig. 6, the time-on-stream experiments revealed that TZ-1 and FTZ catalysts exhibit relatively stable catalytic activity in comparison to TZ-2 sample. Interestingly, the TZ-2 catalyst exhibited a high conversion than that of TZ-1 sample. However, a relatively fast decrease in the conversion is noted for TZ-2 sample due to deactivation of the catalyst owing to coke formation. The coke formation was confirmed by an increase in the weight of the sample and change of its color after the catalytic experiment. The

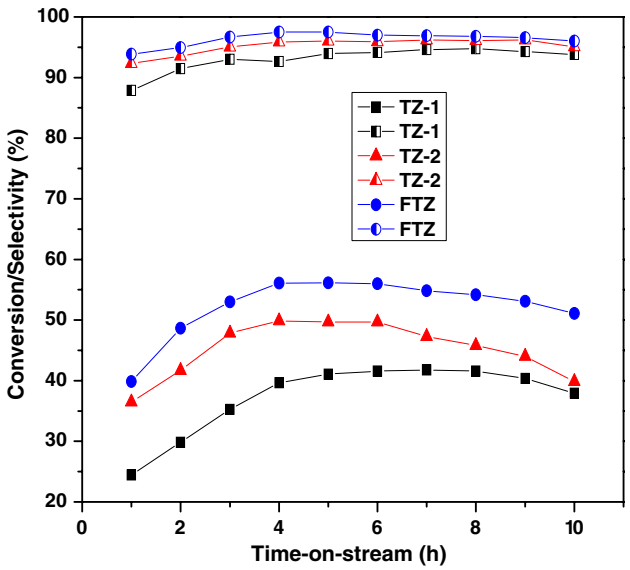

Fig. 6 Variation of catalytic activity and selectivity with time-on-stream over TiO_2–ZrO_2 (TZ-1), TiO_2–ZrO_2 (TZ-2) and Fe_2O_3/TiO_2–ZrO_2 (FTZ) samples at 600 °C and normal atmospheric pressure

activity and selectivity results revealed a good catalytic efficiency of FTZ combination, which exhibited a high and stable activity without rapid deactivation.

To understand the potential role of CO_2 in directing the product formation and catalyst stability, we have investigated various samples for their activity and selectivity in the presence and absence of CO_2 [23, 29]. As noticed earlier, the conversion and selectivity were slightly lower in the first 2–3 h of the reaction and increased thereafter. A significant difference in the EB conversion, styrene selectivity and catalyst stability were noted in the presence (CO_2) and absence (N_2) of CO_2 feed gas inline with previous studies [23, 29]. As elaborated elsewhere [5, 6], a simple dehydrogenation of EB takes place in the absence of CO_2 (Eq. 1) and the reverse water-gas-shift (RWGS) reaction (Eq. 2) coupled with the simple dehydrogenation operates in the presence of CO_2 as shown in Eqs. 1 and 2.

$$C_6H_5CH_2 - CH_3 \rightarrow C_6H_5CH = CH_2 + H_2(\text{dehydrogenation}) \quad (1)$$

$$H_2 + CO_2 \rightarrow CO + H_2O(\text{RWGS}) \quad (2)$$

As advocated by Cavani and Trifiro [10], the oxidation of hydrogen by CO_2 shifts the dehydrogenation equilibrium to achieve higher yields by increasing both conversion and product selectivity. Similar observations were also made by Sun et al. [30] and Liu et al. [31] in their recent studies, and explained the role of CO_2 in coupling the RWGS reaction with EB dehydrogenation. Several investigations also emphasized the significance of reaction mechanism in the presence of CO_2 where redox sites operate either with single step pathway (Eq. 3) or dual step pathway (Eqs. 3 and 4). More details on these mechanisms have been elaborated in our previous publications [4–6].

$$C_6H_5CH_2 - CH_3 + CO_2 \rightarrow C_6H_5CH = CH_2 + H_2O \quad (3)$$

$$C_6H_5CH_2 - CH_3 \rightarrow C_6H_5CH = CH_2 + H_2 \quad (4)$$

The catalytic activity and selectivity results from the present study reveal that iron oxide incorporated chloride containing titania–zirconia composite oxide exhibits a stable catalytic activity with high conversion and product selectivity. As per the literature, the metal chloride species exhibit redox properties [28]. Therefore, the redox properties coupled with acid–base characteristics are expected to play an important role to the observed high activity and selectivity of the catalyst.

4 Conclusions

The following conclusions can be drawn from this investigation: (1) The presence of chloride ions in TiO_2–ZrO_2 mixed oxides influence greatly on the specific surface area,

crystallization and acid–base properties. The chloride free TiO_2–ZrO_2 exhibited a high specific area than chloride containing sample. The chloride containing TiO_2–ZrO_2 sample revealed the presence of relatively strong acidic and weak basic sites as determined by NH_3 and CO_2 TPD measurements, respectively. Further, the chloride containing TiO_2–ZrO_2 mixed oxide exhibited better conversion and product selectivity. (2) The TiO_2–ZrO_2 composite oxide is an interesting carrier for the dispersion of iron oxide. As revealed by XRD and SEM techniques, the deposited iron oxide is in a highly dispersed form over the support surface. The dispersed iron oxide also influenced on the acid–base properties of the mixed oxide support. (3) The combined Fe_2O_3/TiO_2–ZrO_2 catalyst exhibited better catalytic activity and selectivity for the ODH of EB with CO_2 as the oxidant. It can be considered as a promising catalyst for this reaction. Further studies are essential to understand the exact role of chloride ions in the mechanism of EB ODH to styrene in the presence of CO_2.

Acknowledgments This work was supported by Korea Science and Engineering Foundation (KOSEF) grant founded by the Korea Government (MOST) (NRL NO. 36379-1). BMR thanks Korea Federation of Science & Technology (KOFST) for a visiting fellowship under Brain Pool program.

References

1. Smalley R (2003) Energy & nanotechnology conference, Rice University, Houston, USA, 3 May 2003
2. Paul J, Pradier C-M (eds) (1994) Carbon dioxide chemistry: environmental issues. Royal Society of Chemistry, Cambridge, UK, p 405
3. Park S-E, Chang J-S, Lee K-W (eds) (2004) Carbon dioxide utilization for global sustainability, Stud Surf Sci Catal, vol 153. Elsevier, Amsterdam, p xiii
4. Park S-E, Han S-C (2004) J Ind Eng Chem 7:1257–1269
5. Chang J-S, Hong D-Y, Vislovskiy VP, Park S-E (2007) Catal Surv Asia 11:59–69
6. Reddy BM, Han D-S, Jiang N, Park S-E (2008) Catal Surv Asia 12:1–14
7. Lee LH (1973) Catal Rev Sci Eng 8:285–305
8. Cavani F, Trifiro F (1995) Appl Catal A Gen 133:219–239
9. Kochloefl K (1998) In: Ertl G, Knözinger H, Weitkamp J (eds) Handbook of heterogeneous catalysis, vol 5. VCH, Weinhein, p 2151
10. Bhasin MM, McCain JH, Vora BV, Imai T, Pujado PR (2001) Appl Catal A Gen 221:397–419
11. Adams CR, Jennings TJ (1970) J Catal 17:157–177
12. Chang WS, Chen YZ, Yang BL (1995) Appl Catal A Gen 124:221–243
13. Mimura N, Takahara I, Saito M, Hattori T, Ohkuma K, Ando M (1998) Catal Today 45:61–64
14. Shiju NR, Anilkumar M, Mirajkar SP, Gopinath CS, Rao BS, Satyanarayana CVV (2005) J Catal 230:484–492
15. Reddy BM, Rao KN, Reddy GK, Khan A, Park S-E (2007) J Phys Chem C 111:18751–18758
16. Sugino M, Shimada H, Turuda T, Miura H, Ikenaga N, Suzuki T (1995) Appl Catal A Gen 121:125–137
17. Yoo JS (1998) Catal Today 41:409–432
18. Chen S, Qin Z, Sun A, Wang J (2006) J Nat Gas Chem 15:11–20
19. Sakurai Y, Suzaki T, Nakagawa K, Ikenaga N, Aota H, Suzuki T (2002) J Catal 209:16–24
20. Dziembaj R, Kustrowski P, Chmielarz L (2003) Appl Catal A Gen 255:35–44
21. Saito M, Kimura H, Mimura N, Wu J, Murata K (2003) Appl Catal A Gen 239:71–77
22. Carja G, Nakamura R, Aida T, Niiyama H (2003) J Catal 218:104–110
23. Burri DR, Choi K-M, Han S-C, Burri A, Park S-E (2007) Bull Korean Chem Soc 28:53–58
24. Burri DR, Choi K-M, Han S-C, Burri A, Park S-E (2007) J Mol Catal A Chem 269:58–63
25. Reddy BM, Khan A (2005) Catal Rev Sci Eng 47:257–296
26. Reddy BM (2006) In: Fierro JLG (ed) Metal oxides: chemistry and applications, Chapter 8. Taylor & Francis, Florida, pp 215–246
27. Berteau P, Delmon B (1989) Catal Today 5:121–137
28. Choudhary VR, Jana SK (2002) J Mol Catal A Chem 180:267–276
29. Burri DR, Choi K-M, Han S-C, Sujandi, Jiang N, Burri A, Park S-E, Catal Today 131 (2008) 173–178
30. Sun A, Qin Z, Chen S, Wang J (2004) J Mol Catal Chem 210:189–195
31. Liu BS, Rui G, Chang RZ, Au CT (2008) Appl Catal A Gen 335:88–94